Lattice vibration modes in type-II superlattice InAs/GaSb with no-common-atom interface and overlapping vibration spectra

Henan Liu,[1] Naili Yue,[2] Yong Zhang,[1,2,*] Pengfei Qiao,[3] Daniel Zuo,[3] Ben Kesler,[3] Shun Lien Chuang,[3] Jae-Hyun Ryou,[4] James D. Justice,[4] and Russell Dupuis[4]

[1]*Optical Science and Engineering Graduate Program, University of North Carolina at Charlotte, Charlotte, North Carolina, USA*
[2]*Department of Electrical and Computer Engineering, University of North Carolina at Charlotte, Charlotte, North Carolina, USA*
[3]*Department of Electrical and Computer Engineering, University of Illinois at Urbana-Champaign, Champaign, Illinois USA*
[4]*Center for Compound Semiconductors and School of Electrical and Computer Engineering, Georgia Institute of Technology, Atlanta, Georgia, USA*

(Received 1 February 2015; published 24 June 2015)

Heterostructures like InAs/GaSb superlattices (SLs) are distinctly different from well-studied ones like GaAs/AlAs SLs in terms of band alignment, common interface atom, and phonon spectrum overlapping of the constituents, which manifests as stark differences in their electronic and vibrational properties. This paper reports a comprehensive examination of all four types of phonon modes (confined, quasiconfined, extended, and interface) that have long been predicted for the InAs/GaSb SL, with the observation and interpretation of a set of phonon modes by performing cleaved edge μ-Raman study with polarization analysis. Furthermore, we show a signature of symmetry reduction from D_{2d} for GaAs/AlAs SL to C_{2v} for InAs/GaSb SL revealed as a phonon-polariton effect.

DOI: 10.1103/PhysRevB.91.235317 PACS number(s): 78.30.Fs, 63.20.kk, 63.22.Np, 78.67.Pt

I. INTRODUCTION

InAs and GaSb form an unusual type of heterostructure: type II band alignment with a broken bandgap, no-common-atom interfaces, and overlapping optical phonon spectra, in contrast to better studied heterostructures, such as of GaAs and AlAs with type I band alignment, common-anion interfaces, and nonoverlapping optical phonon spectra [1]. These differences make the electronic structure and vibration spectrum of InAs/GaSb heterostructure more complex and intriguing as well as less well understood. Besides using InAs/GaSb type II superlattices (T2SLs) for infrared (IR) detection [2,3], InAs/GaSb heterostructures have lately been explored for fundamental interests, such as exciton condensation [4,5], the quantum spin Hall effect or topologic insulator [6–10], and a graphenelike Dirac fermion [11].

Raman spectroscopy is widely used for studying lattice vibrations and probing electron-phonon coupling in semiconductor SLs [12]. The observation of confined phonons in GaAs/AlAs SLs provides not only an indication of high structural quality but also valuable information for the bulk vibration spectra [12]. The optical phonon spectra of InAs and GaSb strongly overlap [13]. For longitudinal optical (LO) phonons, the Γ-X dispersion of InAs (238.6–203 cm^{-1}) encloses that of GaSb (233.1–211.4 cm^{-1}); for transverse optical (TO) phonons, that of GaSb (228.8–211.8 cm^{-1}) encloses InAs (217.3–216 cm^{-1}). The phonon spectrum of the T2SL has been predicated to have four types of modes: confined (C), quasiconfined (QC), extended (EX), and interface (IF) modes [13–16]. No-common-element IF has two consequences: (1) two IF modes, GaAs-like (IF1) and InSb-like (IF2), located above and below the general SL modes [13,16]; and (2) the reduction of the SL symmetry from D_{2d} for GaAs/AlAs SLs to C_{2v} for InAs/GaSb SLs [16]. One important point that has not previously received attention is that the Raman cross sections (RCs) of the two constituents are very different for the T2SL, which turns out to be pivotal for understanding its Raman spectrum.

Numerous Raman studies of T2SLs have been reported [17–24]. Most of them were performed in the (001) backscattering geometry, with only one major Raman peak observed at around 236−238 cm^{-1} assigned generally as a SL-LO mode. It was believed that the overlapping of the bulk phonon modes would make it difficult to resolve the C and EX modes [18–20]. Two weak LO-IF modes have also been reported and are often used to assess the IF composition [22]. An attempt has been made to perform the cleaved edge Raman study on T2SLs but failed to resolve the SL signal from that of the substrate [21]. In short, except for the IF modes, previous efforts on T2SLs have not been able to make any unambiguous connection between the experimental results and the theoretical predictions.

In this paper, we conduct a micro-Raman study of a series of InAs/GaSb SL samples grown on either InAs or GaSb substrate and thick InAs and GaSb epilayers, from both the (001) growth plane and (110) or ($\bar{1}$10) cleaved edges in backscattering geometry. By performing selection rule analyses and direct comparison with the "bulk" references, we (1) conclude that the previously reported SL-LO phonon mode was a GaSb QC-LO mode and that the anticipated InAs C mode is not observable due to a small InAs RC; (2) observe a set of new TO Raman lines with characteristics of QC, EX, and IF modes. The use of two types of substrates and two "bulk" reference samples is critical for making the Raman mode assignments, because changing the substrate is equivalent to applying strain to the SL, and making a direct comparison between the bulk and SL samples can assess their relative RCs. This paper experimentally reveals the signatures of the unique vibration spectrum of the T2SL and thus provides benchmark data for testing the theory. The derived information about the electron-phonon coupling will be critical to assess recently proposed quantum transport applications that

*yong.zhang@uncc.edu

are ultimately determined by the electron-phonon interaction [25,26].

II. EXPERIMENT

Four metal organic chemical vapor deposition (MOCVD) samples were grown on (001) InAs substrates [27], with InAs/GaSb layers in nm as 5/3.1 (labeled as G22), 4.8/3 (G30), 5.45/2.43(G54), and 5.14/2.43 (G55). The total SL thicknesses are 2.4–2.5 μm, except for G22 being $\sim$0.4 μm. No intentional interfacial treatment was applied during growth of these SLs, so both GaAs and InSb interfaces [with GaAs and InSb bonds in the (110) plane] were possible (known as "neutral" interface). Two molecular beam epitaxy (MBE) samples (IFA and IFRA) were grown on GaSb substrates, with InAs/GaSb layers as 4.5/2.4, total SL thicknesses of 3.1–3.2 μm, and 20 nm InAs and 5 nm GaSb caps [28]. They differ in the interfacial treatments, with neutral IFs in IFA and only InSb IFs in IFRA. The results of the MOCVD samples are qualitatively similar. Most results presented are from G54 and IFA, unless noted otherwise. InAs and GaSb bulk samples, about 1 μm thick, were grown by MOCVD on their native substrates. They are slightly lattice mismatched with $a_{\mathrm{InAs}} : a_{\mathrm{GaSb}} \approx 1 : 1.007$. Because of the small lattice mismatch, the SL is coherently strained to the substrate on the growth plane; i.e., the GaSb layers of the SL are under in-plane compressive strain when grown on InAs substrate and the InAs layers of the SL under tensile strain when grown on GaSb substrate. Raman measurements were conducted at room temperature, using a Horiba HR800 confocal Raman microscope with a charge-coupled device (CCD) detector and a 100$\times$ microscope lens (NA = 0.9). The spectral dispersion is 0.44 cm^{-1}/pixel, and the spatial resolution is $\sim$0.36 μm using a 532 nm laser. The spectrometer was calibrated to yield the Si Raman peak at 520.7 cm^{-1}. Sufficiently low laser power ($\sim$0.3 mW) was used to avoid sample heating. This precaution is vitally important: Because the thermal conductivities of the bulk and SL samples are rather different, heating can cause significantly different line shifts for different modes and thus confusion in assigning Raman modes.

III. RESULTS AND DISCUSSION

For C_{2v} symmetry, there are four allowed Raman modes with these Raman tensors [29]: $A_1(z') = [(a,0,0), (0,b,0), (0,0,c)]$, $B_1(x') = [(0,0,e), (0,0,0), (e,0,0)]$, $B_2(y') = [(0,0,0), (0,0,f), (0,f,0)]$, and $A_2 = [(0,d,0),(d,0,0), (0,0,0)]$. Here x', y', and $z\prime$ are the principal axes with $x' \sim (110)$, $y' \sim (\bar{1}10)$, and $z' \sim (001)$, with respect to the cubic axes $x \sim (100)$, $y \sim (010)$, and $z \sim (001)$. If one envisions that the difference between either the cations or the anions vanishes, D_{2d} symmetry should be recovered. Indeed, by letting $a = b$, $c = 0$, and $e = f$, A_1 and (B_1,B_2) will become $B_2(z)$ and $E(x,y)$ of D_{2d}, respectively. A_2 does not have a correspondence in D_{2d}. Thus, c and d are entirely due to the symmetry reduction from D_{2d} to C_{2v}, and their effects are expected to be small. The key C_{2v} Raman selection rules are summarized in Table I, by calculating the Raman intensity $\propto |\mathbf{e}_i \cdot \mathrm{R} \cdot \mathbf{e}_s|^2$, where R is the Raman tensor and $\mathbf{e}_i$ and $\mathbf{e}_s$ are the polarization vectors of the incident and scattered light.

TABLE I. Polarization selection rules for C_{2v} Raman modes in backscattering geometries with photon wave vectors along $z' \sim [001]$, $x' \sim [110]$, and $y' \sim [\bar{1}10]$. The results for two cross-polarizations are identical, and only one is shown.

Symmetry geometry	$A_1(z')$	$B_1(x')$	$B_2(y')$
$z'(x',x')\bar{z}'$	a^2_{LO}	0	0
$z'(y',y')\bar{z}'$	b^2_{LO}	0	0
$z'(x',y')\bar{z}'$	0	0	0
$x'(y',y')\bar{x}'$	b^2_{TO}	0	0
$y'(x',x')\bar{y}'$	a^2_{TO}		
$x'(z',z')\bar{x}'$	c^2_{TO}	0	0
$y'(z',z')\bar{y}'$			
$x'(y',z')\bar{x}'$	0	e^2_{TO}	f^2_{TO}
$y'(x',z')\bar{y}'$			

A. (001) Backscattering

Figure 1 compares Raman spectra with different polarization configurations for four samples, T2SL G54 and IFA, InAs, and GaSb, obtained under the same conditions. Only the results of $z(x',x')\bar{z}$ and $z(x',y')\bar{z}$ are shown, because the others are qualitatively similar. First, evidently the RC of GaSb is substantially larger than that of InAs ($\sim$5 : 1), implying that InAs-like modes are less observable in the SL, which is an important clue for identifying Raman modes. Second, the primary SL peak is found at $\sim$238.6 cm^{-1} or $\sim$234.3 cm^{-1} in the T2SLs, respectively, on InAs and GaSb. The peak position varies only slightly within the SL samples on the same substrate (less than 0.5 cm^{-1}) but greatly with changing substrate, because of the epitaxial strain. The SL mode in the SL on GaSb matches the predicted GaSb QC-LO mode at a wave number slightly below the GaSb LO mode [14,16]. For the SL on InAs, despite being close to the InAs LO, the SL mode is in fact the same GaSb QC-LO mode but blueshifted due to the compressive strain. Furthermore, the SL mode in the InAs-substrate sample shows an intensity between those of the bulk GaSb and InAs, which is consistent with its assignment as a GaSb QC-LO mode, because the lowest order consideration based on the volume would suggest the intensity to be simply determined by the fraction of GaSb in the SL. If it were an InAs LO like mode, the intensity would be below that of the bulk InAs. The lower intensity of the SL mode for the GaSb-substrate sample is due to the absorption of its cap layers. The weaker peak at $\sim$228 cm^{-1} in the SL on InAs or $\sim$226 cm^{-1} in the SL on GaSb could be due to the forbidden GaSb derived TO mode. However, given the larger width of the peak and the enhanced relative intensity when compared to the primary LO mode, in particular for the SL on GaSb, this peak might also contain unresolved EX modes. The predicted InAs confined modes [15,16] are not observed, likely due to the small RC of InAs bulk. We also examined the potential anisotropy between x' and y', i.e., a_{LO} vs b_{LO}, and find that the difference, if any, is less than 1% (within the uncertainty). In summary, the primary SL-LO Raman mode measured on the growth plane is a GaSb QC-LO mode with A_1 symmetry.

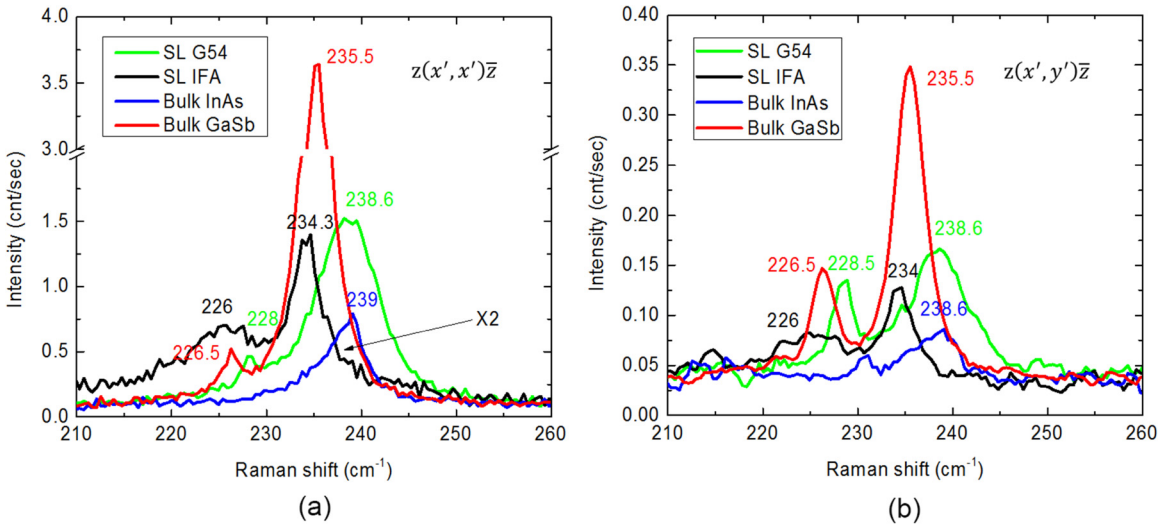

FIG. 1. (Color online) (001) backscattering Raman spectra of InAs/GaSb SLs, compared with those of InAs and GaSb thick epilayers in two polarization configurations: (a) $z(x',x')\bar{z}$ and (b) $z(x',y')\bar{z}$.

B. (110) and ($\bar{1}$10) cleaved edge backscattering

First we demonstrate in Fig. 2 the ability to unambiguously resolve the SL Raman signal from the substrate on the cleaved edge using sample G55. Figure 2(a) shows an optical image of the cleaved edge under white light illumination, showing a visible optical contrast between the SL and substrate. Figures 2(b) and 2(c) are Raman mapping results on the cleaved edge for two modes: ~226 cm^{-1}, a SL EX-TO mode that is seen only in the SL epilayer region, and ~217.5 cm^{-1}, an InAs QC-TO mode of the SL at nearly the same frequency as that of the bulk InAs TO mode, showing uniform intensity across the SL/substrate boundary. Below we discuss the Raman mode assignments by applying polarization analyses and comparing with the bulk references.

Figure 3 shows typical results for the two SL samples, respectively, on InAs and GaSb substrate, compared directly with the bulk references. For T_d symmetry, the TO mode is allowed

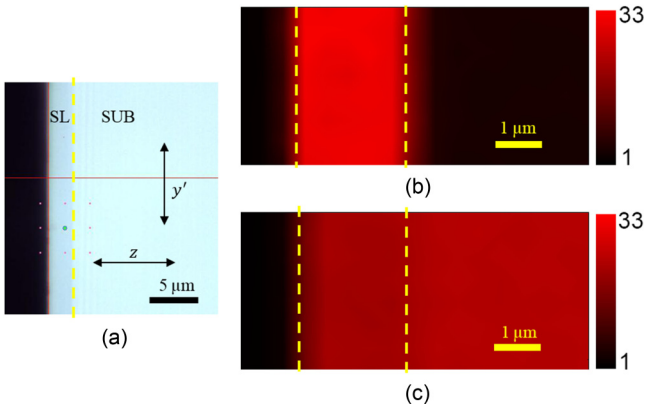

FIG. 2. (Color online) Raman mapping from the (110) cleaved edge of an InAs/GaSb SL grown on InAs substrate, showing the ability to resolve unambiguously the signal from the SL and substrate. (a) Optical image under white light illumination, (b) Raman mapping result in $x'(y',z)\bar{x}'$ for a SL mode at ~226 cm^{-1} that does not exist in the substrate, and (c) the same as (b) but for an InAs like SL mode at ~217 cm^{-1} that also exists in the substrate.

in three equivalent configurations, $x'(y',z)\bar{x}'$, $x'(z,y')\bar{x}'$, and $x'(y',y')\bar{x}'$, but forbidden in $x'(z,z)\bar{x}'$ [30]. This is confirmed in Fig. 3 for the bulk samples, showing a TO mode at 226.5 cm^{-1} and a (weak) LO mode at ~236 cm^{-1} for GaSb and a TO mode at 217.4 cm^{-1} for InAs. The GaSb RC is again much larger than InAs (~14 : 1). For SLs, the spectra of $x'(y',z)\bar{x}'$ and $x'(z,y')\bar{x}'$ are essentially the same, as shown in Figs. 3(a) and 3(b), with two major peaks: 226 cm^{-1} and ~217.8 cm^{-1} for the SL on InAs and 224.3 cm^{-1} and ~216.5 cm^{-1} for the SL on GaSb. The Raman selection rules indicate that these modes should have $B_2(y')$ symmetry. The lower frequency mode can be assigned as an InAs QC-TO mode based on its frequency in the SL sample on InAs as well as its intensity being lower than the bulk InAs. The higher frequency mode should be assigned as an EX-TO mode rather than an expected GaSb C-TO [13,16], based on two considerations: (1) its intensity is about 1/8 of the bulk GaSb, while the GaSb volume fraction is about 1/3; and (2) the frequency difference with respect to the bulk GaSb TO for the SL sample on GaSb is significantly larger than those of calculated GaSb QC or C modes [7,10]. Here again we observe the strain effect: for the SL on InAs, the EX-TO mode is blueshifted (incidentally matching the TO mode of the bulk GaSb) due to the compressive strain; for the SL on GaSb, the InAs QC-TO mode is redshifted due to the tensile strain. The InAs QC-TO mode is less sensitive to the strain than the GaSb QC-LO mode, which is consistent with the strain effects in the bulks [31,32].

For $x'(y',y')\bar{x}'$, shown in Fig. 3(c), three additional peaks are observed: 221, 237, and 250 cm^{-1} for the SL on InAs, and 219.5, 234, and ~245 cm^{-1} for the SL on GaSb. Again these are the same set of Raman modes but shifted against each other due to the epitaxial strain. The Raman selection rules indicate that these modes should have $A_1(z)$ symmetry. The lowest frequency mode at 221 or 219.5 cm^{-1} can be attributed to an EX-TO mode, with both its intensity and frequency falling between the two bulk TO modes. Because this mode is derived from the bulk TO modes, there is not an obvious A_1 LO counterpart in the (001) backscattering

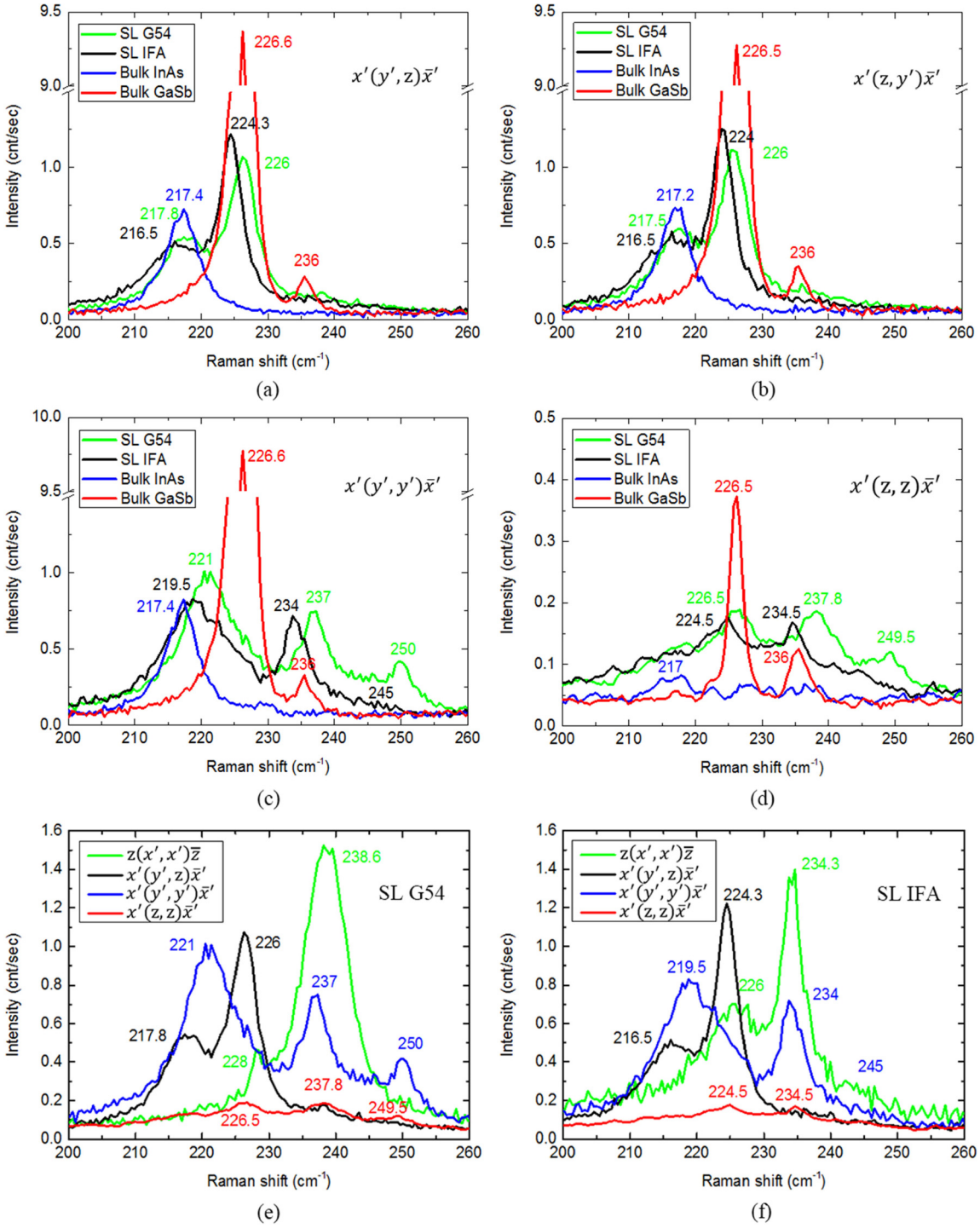

FIG. 3. (Color online) (110) backscattering Raman spectra for the same samples as in Fig. 1. (a–d) Comparison of the four samples in four polarization configurations, (a) $x'(y',z)\bar{x}'$, (b) $x'(z,y')\bar{x}'$, (c) $x'(y',y')\bar{x}'$, and (d) $x'(z,z)\bar{x}'$. (e, f) the comparison of one SL sample under different polarization configurations, respectively, for the SL on InAs and GaSb substrate.

measurement. In fact, it is a broad band that appears to comprise unresolved components on the high frequency side. By deconvoluting this broadened peak into two components, we get another weak peak at ∼227 or 224 cm^{-1} that is close to the B_2 symmetry EX-TO mode observed in $x'(y',z)\bar{x}'$ but forbidden in $x'(y',y')\bar{x}'$. The highest frequency mode at 250 or ∼245 cm^{-1} is close to the predicted GaAs IF_1-TO mode with A_1 symmetry [13]. However, the LO counterpart for this IF mode is not well resolved in the (001) backscattering, indicating that the cleaved edge has higher sensitivity for probing the IF mode. The behavior of the middle mode is peculiar: Its frequency 237 or 234 cm^{-1} is above all the bulk TO modes and in fact rather close to the GaSb QC-LO mode at 238.6 or 234.3 cm^{-1}, but its intensity is much stronger than the forbidden bulk GaSb LO and actually comparable to the EX-TO modes. Additionally, the strain shift of this mode is

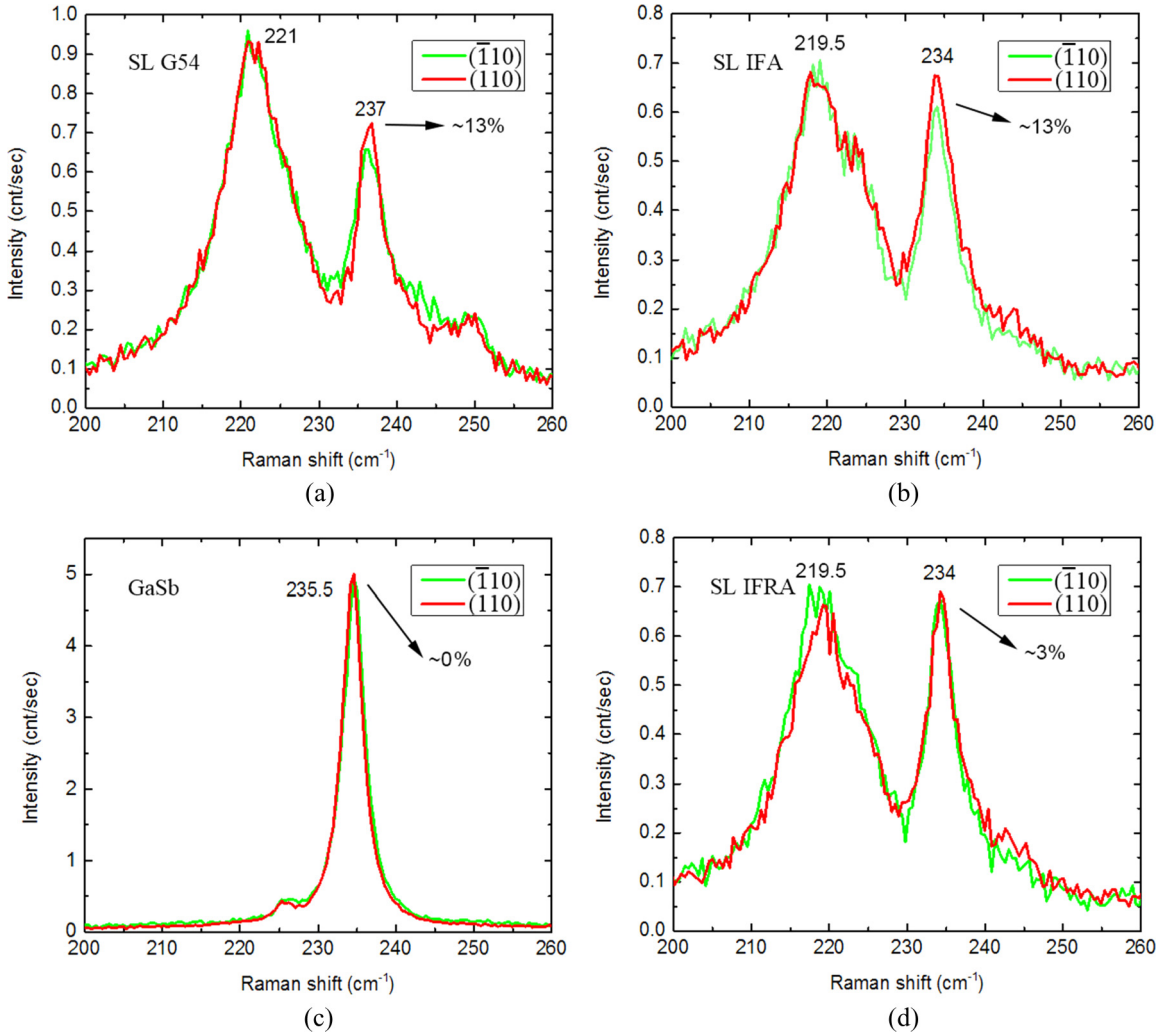

FIG. 4. (Color online) The comparison of Raman spectra measured from two cleaved edges (110) and ($\bar{1}$10). (a) SL G54 (neutral-IF SL on InAs), (b) SL IFA (neutral-IF SL on GaSb), (c) thick GaSb epilayer, and (d) SL IFRA (SL with only InSb IFs on GaSb).

substantially larger than those TO-type modes. Apparently, this mode cannot be readily assigned as any of the predicted SL modes [7–10]. It should be interpreted as a transverse counterpart of the GaSb QC-LO with A_1 symmetry split due to the phonon-polariton effect. It is also the only mode showing observable anisotropy between x' and y', to be discussed later.

For $x'(z,z)\bar{x}'$, as shown in Fig. 3(d), two weak modes were resolved: ~226.5 cm^{-1} and ~237.8 cm^{-1} in SL on InAs and ~224.5 cm^{-1} and ~234.5 cm^{-1} in SL on GaSb. This configuration is forbidden for all the modes belonging to T_d or D_{2d} symmetry, but allowed for the $A_1(z)$ mode of C_{2v} symmetry due to the c component of $A_1(z)$ induced by symmetry lowering. Therefore, these modes could either arise from the anticipated weak $A_1(z)$ or be the vestiges of the EX-TO modes observed in $x'(y',z)\bar{x}'$ and $x'(y',y')\bar{x}'$. Figures 3(e) and 3(f) compare (001) and the cleaved edge spectra for the four distinct polarization configurations, respectively, for the two SL samples to highlight the relative positions and intensities of different modes.

So far we have discussed the results from one cleaved edge, assumed to be (110). We now examine the possible anisotropy between $x'(y',y')\bar{x}'$ and $y'(x',x')\bar{y}'$ expected for C_{2v} [22]. By mounting two cleaved edge pieces of (110) and ($\bar{1}$10) side by side and measuring them under the same conditions, we can detect anisotropy on the order of 1%. We have found only one SL Raman mode, 237 cm^{-1} (G54) or 234 cm^{-1} (IFA), that exhibits significant intensity anisotropy ~13% between (110) and ($\bar{1}$10), as shown in Figs. 4(a) and 4(b). On the same spectrum, the ~221 or ~219.5 cm^{-1} peak, shows no apparent anisotropy. To further confirm the reliability, the bulk GaSb is shown to be indeed isotropic, Fig. 4(c), and the sample with modified interface IFRA exhibits substantially reduced anisotropy ~3%, Fig. 4(d). Therefore, we may conclude that the effect of symmetry reduction from D_{2d} to C_{2v} is minimal for most situations, nevertheless observable for certain modes. This anisotropy is another indication of the phonon-polariton nature of this mode that alters the basic Raman selection rule.

IV. SUMMARY

In summary, we have concluded that the previously reported Raman mode observed in the (001) backscattering is a GaSb QC-LO mode with A_1 symmetry. From the (110) or ($\bar{1}$10) cleaved edge, we have observed at least five new Raman

modes: one EX-TO and one InAs QC-TO mode with B_2 or B_1 symmetry, one EX-TO, one IF_1-TO, and a phonon-polariton TO mode associated with the GaSb QC-LO mode, all with A_1 symmetry. The phonon-polariton mode shows anisotropy between the (110) or $(\bar{1}10)$ plane, expected for a structure with C_{2v} biaxial symmetry. All the other modes behave as though having D_{2d} uniaxial symmetry. No predicted confined mode has been observed, suggesting the need for an improved lattice dynamics theory.

ACKNOWLEDGMENTS

This paper has been supported by the Multidisciplinary University Research Initiative (MURI) program (under the supervision of Dr. William Clark) from the US Army Research Laboratory and the US Army Research Office under Grant No. Army W911NF-10-1-0524. Y.Z. acknowledges the support of the Bissell Distinguished Professorship.

[1] H. Kroemer, Physica E **20**, 196 (2004).
[2] C. H. Grein, P. M. Young, M. E. Flatte, and H. Ehrenreich, J. Appl. Phys. **78**, 7143 (1995).
[3] E. A. Plis, Adv. Electron. **2014**, 246769 (2014).
[4] Y. Naveh and B. Laikhtman, Phys. Rev. Lett. **77**, 900 (1996).
[5] D. I. Pikulin and T. Hyart, Phys. Rev. Lett. **112**, 176403 (2014).
[6] C. Liu, T. L. Hughes, X.-L. Qi, K. Wang, and S.-C. Zhang, Phys. Rev. Lett. **100**, 236601 (2008).
[7] W. Pan, J. F. Klem, J. K. Kim, M. Thalakulam, M. J. Cich, and S. K. Lyo, Appl. Phys. Lett. **102**, 033504 (2013).
[8] K. Suzuki, Y. Harada, K. Onomitsu, and K. Muraki, Phys. Rev. B **87**, 235311 (2013).
[9] I. Knez, C. T. Rettner, S.-H. Yang, S. S. P. Parkin, L. Du, R.-R. Du, and G. Sullivan, Phys. Rev. Lett. **112**, 026602 (2014).
[10] P. C. Klipstein, Phys. Rev. B **91**, 035310 (2015).
[11] J. B. Khurgin and I. Vurgaftman, Appl. Phys. Lett. **104**, 132107 (2014).
[12] J. Menéndez, J. Luminescence **44**, 285 (1989).
[13] A. Fasolino, E. Molinari, and J. C. Maan, Phys. Rev. B **33**, 8889 (1986).
[14] A. Fasolino, E. Molinari, and J. C. Maan, Superlattices Microst. **3**, 117 (1987).
[15] A. Fasolino, E. Molinari, and J. C. Maan, Phys. Rev. B **39**, 3923 (1989).
[16] D. Berdekas and G. Kanellis, Phys. Rev. B **43**, 9976 (1991).
[17] C. Lopez, R. J. Springett, R. J. Nicholas, P. J. Walker, N. J. Mason, and W. Hayes, Surf. Sci. **267**, 176 (1992).
[18] I. Sela, L. A. Samoska, C. R. Bolognesi, A. C. Gossard, and H. Kroemer, Phys. Rev. B **46**, 7200 (1992).
[19] J. R. Waterman, B. V. Shanabrook, R. J. Wagner, M. J. Yang, J. L. Davis, and J. P. Omaggio, Semicond. Sci. Technol. **8**, S106 (1993).
[20] M. Inoue, M. Yano, H. Furuse, N. Nasu, and Y. Iwai, Semicond. Sci. Technol. **8**, S121 (1993).
[21] D. Behr, J. Wagner, J. Schmitz, N. Herres, J. D. Ralston, P. Koidl, M. Ramsteiner, L. Schrottke, and G. Jungk, Appl. Phys. Lett. **65**, 2972 (1994).
[22] S. G. Lyapin, P. C. Klipstein, N. J. Mason, and P. J. Walker, Phys. Rev. Lett. **74**, 3285 (1995).
[23] N. Herres, F. Fuchs, J. Schmitz, K. M. Pavlov, J. Wagner, J. D. Ralston, P. Koidl, C. Gadaleta, and G. Scamarcio, Phys. Rev. B **53**, 15688 (1996).
[24] L.-G. Li, S.-M. Liu, S. Luo, T. Yang, L.-J. Wang, F.-Q. Liu, X.-L. Ye, B. Xu, and Z.-G. Wang, Nanoscale Res. Lett. **7**, 160 (2012).
[25] F. Rossi and T. Kuhn, Rev. Mod. Phys. **74**, 895 (2002).
[26] A. Thränhardt, S. Kuckenburg, A. Knorr, T. Meier, and S. W. Koch, Phys. Rev. B **62**, 2706 (2000).
[27] Y. Huang, J.-H. Ryou, R. D. Dupuis, D. Zuo, B. Kesler, S.-L. Chuang, H.-F. Hu, K.-H. Kim, Y. T. Lu, K. C. Hsieh, and J.-M. Zuo, Appl. Phys. Lett. **99**, 011109 (2011).
[28] D. Zuo, P. F. Qiao, D. Wasserman, and S. L. Chuang, Appl. Phys. Lett. **102**, 141107 (2013).
[29] R. Loudon, Adv. Phys. **13**, 423 (1964).
[30] P. Yu and M. Cardona, *Fundamentals of Semiconductors*, 4th ed. (Springer, New York, 2010).
[31] B. Jusserand, P. Voisin, M. Voos, L. L. Chang, E. E. Mendez, and L. Esaki, Appl. Phys. Lett. **46**, 678 (1985).
[32] M. J. Yang, R. J. Wagner, B. V. Shanabrook, W. J. Moore, J. R. Waterman, C. H. Yang, and M. Fatemi, Appl. Phys. Lett. **63**, 3434 (1993).